TTP09-10
SFB/CPP-09-31
April 2009

Probing Yukawa Unification with K and B Mixing

Stéphanie Trine[1], Susanne Westhoff[1], and Sören Wiesenfeldt[1,2]

[1] *Institut für Theoretische Teilchenphysik, Universität Karlsruhe, 76128 Karlsruhe, Germany*
[2] *Helmholtz Association, Anna-Louisa-Karsch-Straße 2, 10178 Berlin, Germany*

Abstract

We consider corrections to the unification of down-quark and charged-lepton Yukawa couplings in supersymmetric GUTs, which links the large $\nu_\tau - \nu_\mu$ mixing angle to $b \to s$ transitions. These corrections generically occur in simple grand-unified models with small Higgs representations and affect $s \to d$ and $b \to d$ transitions via the mixing of the corresponding right-handed superpartners. On the basis of a specific SUSY-SO(10) model, we analyze the constraints from $K - \overline{K}$ and $B_d - \overline{B_d}$ mixing on the additional $\tilde{d}_R - \tilde{s}_R$ rotation angle θ. We find that ϵ_K already sets a stringent bound on θ, $\theta^{\max} \sim \mathcal{O}(1^\circ)$, indicating a very specific flavor structure of the correction operators. The impact of the large neutrino mixings on the unitarity triangle analysis is also briefly discussed, as well as their ability to account for the sizeable CP-violating phase observed recently in $B_s \to J/\psi\phi$ decays.

1 Introduction

The start of the LHC at CERN will enable us to study TeV-scale physics directly for the first time. Most importantly, we will eventually probe the mechanism of electroweak symmetry breaking; moreover, we will be able to test various scenarios for new physics beyond the standard model (SM), the leading candidate of which is arguably supersymmetry (SUSY). The presence of supersymmetry at the TeV-scale eliminates the quadratically-divergent loop contributions to the Higgs mass and thereby stabilizes the electroweak scale against the scales of more fundamental physics. In addition, TeV-scale SUSY models provide an attractive mechanism for electroweak symmetry breaking and an appealing candidate for cold dark matter. Furthermore, they offer a compelling outline for the unification of all matter and interactions, the first step of which is grand unification [1].

The near unification of the SM gauge couplings within the minimal supersymmetric standard model (MSSM) at $M_{\rm GUT} \simeq 2 \cdot 10^{16}$ GeV, with the MSSM being valid above the TeV-scale, suggests that the standard-model group, $\mathrm{G_{SM}} = \mathrm{SU(3)}_C \times \mathrm{SU(2)}_L \times \mathrm{U(1)}_Y$, is embedded into a simple gauge group at this scale, such as SU(5) [2] or SO(10) [3]. SO(10) is arguably the most natural GUT group: both the SM gauge and matter fields are unified, introducing only one additional matter particle, the right-handed neutrino.[1] It is an anomaly-free theory and therefore explains the intricate cancellation of the anomalies in the standard model [4]. Moreover, it contains $B - L$ as a local symmetry, where B and L are baryon and lepton number, respectively; the breaking of $B - L$ provides light neutrino masses via the seesaw mechanism. Remarkably, $M_{\rm GUT}$ is of the right order of magnitude to generate neutrino masses in the sub-eV range. Hence, the neutrino masses are linked to the breaking of the GUT symmetry [5].

Flavor experiments, though not able to access the TeV scale directly, have put strong constraints on the MSSM parameters. Due to the lack of deviation with respect to the SM, we expect the new sources of flavor mixing and CP violation to be very limited for SUSY particles around the weak scale. As formulated by the concept of minimal flavor violation [6, 7], we assume that the Yukawa couplings

[1] Strictly speaking, it is the left-handed neutrino singlet.

are the only source of flavor violation and (even more) that the supersymmetry breaking parameters are universal at some fundamental scale. Within the minimal supergravity (mSUGRA) scenario [8], this scale is usually taken to be $M_{\rm GUT}$. An alternative and arguably more natural choice, however, would be the Planck scale, $M_{\rm Pl} = G_N^{-1/2} = 1 \cdot 10^{19}$ GeV.[2] The reason to take the MSSM unification scale instead is simply that while the use of the renormalization group equations of the MSSM below $M_{\rm GUT}$ is undisputed, the analysis of the region between $M_{\rm GUT}$ and $M_{\rm Pl}$ requires knowledge about the grand-unified model. However, the universality of the SUSY-breaking parameters is broken by their evolution down to lower energies. Thus the choice of $M_{\rm GUT}$ eliminates potentially important flavor effects. In our analysis, we will adopt $M_{\rm Pl}$ as universality scale, and study consequences of this choice in detail.

In the standard model, fermion mixing is only measurable among the left-handed states and described by the quark and lepton mixing matrices, $V_{\rm CKM}$ and $V_{\rm PMNS}$. Both small and large mixing angles are realized: while those in the quark sector are small, two angles in $V_{\rm PMNS}$ turn out to be large. These are the neutrino solar and atmospheric mixing angles, where the latter is close to maximal. The effects of $V_{\rm CKM}$ and $V_{\rm PMNS}$ are confined to the quark and to the lepton sectors, respectively. In GUTs, however, this separation of quark and lepton sector is abrogated as quarks and leptons are unified. Thus their masses and mixings are related to each other. While different patterns are possible, it is natural to expect imprints of $V_{\rm PMNS}$ on the quark sector as well. In particular, it might be possible to trade off small rotations of left-handed down quarks and right-handed leptons against large mixings among right-handed down quarks and left-handed leptons, as we will discuss below. The mixing of the right-handed fermions is unobservable due to the absence of right-handed flavor-changing currents at the weak scale. With weak-scale supersymmetry, the mixing of the corresponding scalar partners of quarks and leptons becomes physical.

The impact of the large atmospheric mixing angle on B_s physics has already been investigated in detail [9, 10, 11, 12]. Due to the good agreement of the bottom-quark and tau-lepton masses at $M_{\rm GUT}$, one can adopt the predicted Yukawa unification of down quarks and charged leptons. In order to study K and B_d physics, however, one needs to go beyond minimal models and modify the relations among the Yukawa couplings.[3] Here, we can pursue two avenues: we can either introduce additional Higgs fields in larger representations, such as a 45_H in SU(5), or parameterize the modifications via higher-dimensional operators, suppressed by powers of a more fundamental scale [15]. We opt for the latter route for three reasons. One, large Higgs representations introduce a large number of additional fields, which both yields large threshold corrections at $M_{\rm GUT}$ and makes the gauge coupling blow up shortly above the GUT scale. Two, the use of higher-dimensional operators reflects the successful Yukawa unification of the third generation; the corrections are suppressed and therefore apply mostly to the lighter generations. Finally, we are able to perform a more general study as we do not rely on specific Higgs fields.

In this paper, we will study the impact of the higher-dimensional Yukawa operators on $K - \overline{K}$ and $B_d - \overline{B_d}$ mixing. A SUSY-SO(10) GUT with universal supersymmetry-breaking parameters at the Planck scale will serve as our specific framework. In particular, the precise measurement of ϵ_K will enable us to tightly constrain the additional (s)quark mixing caused by these operators. The validity of our results for more general classes of grand-unified models will also be assessed.

[2] Alternatively, one might choose the *reduced* Planck scale, $M_{\rm Pl} = (8\pi G_N)^{-1/2} = 2 \cdot 10^{18}$ GeV, because it compensates for the factor 8π in the Einstein field equations.

[3] These modifications were neglected in Ref. [13], whose authors consider minimal SU(5). Similarly, Ref. [14] assumes a minimal SO(10) model where $V_{\rm CKM}$ describes all SM flavor mixing (the study is from 1995, i.e. before the large mixing angles in the lepton sector were established).

2 Yukawa Unification and Dimension-five Operators

Grand-unified theories using small Higgs representations to break the electroweak symmetry generically predict the unification of down-quark and charged-lepton masses [1, 2]. [4] Before turning to SO(10), let us consider minimal SU(5) to bring out the central idea of this work. Here the down-quark singlet, d^c, and lepton doublet, L, fill up the $\overline{5}$ representation, whereas the quark doublet, Q, as well as the up-quark and the electron singlets, u^c and e^c, are embedded in the 10. As usual, these are left-chiral superfields; for instance, we have the electron singlet e_L^c instead of the right-handed electron e_R. The adjoint Higgs field Σ breaks SU(5) to the standard-model group, which is then broken to $\mathrm{SU}(3)_C \times \mathrm{U}(1)_{\mathrm{em}}$ by a pair of quintets, $H + \overline{H}$.

The corresponding Yukawa couplings read

$$W_Y = \mathsf{Y}_1^{ij}\, \epsilon_{abcde}\, 10_i^{ab}\, 10_j^{cd}\, H^e + \mathsf{Y}_2^{ij}\, 10_i^{ab}\, \overline{5}_{ja}\, \overline{H}_b \;, \tag{1}$$

where a, $b, \ldots$ denote SU(5) and i, j flavor indices. The second coupling yields the unification of down-quark and charged-lepton Yukawa couplings $\mathsf{Y}_{d,e}$ (and thus of the corresponding masses). If $\mathsf{Y}_{d,e}$ are defined such that the weak doublets are on the left and the singlets on the right, we obtain

$$\mathsf{Y}_d = \mathsf{Y}_e^\top = \mathsf{Y}_2 \;. \tag{2}$$

The mixings of the right-handed (left-handed) down quarks are thus identical (or, more precisely, conjugated) to those of the left-handed (right-handed) charged leptons.

This relation works remarkably well for the third generation but not for the lighter ones. Thus we need to include corrections, which are generically generated by higher-dimensional Yukawa operators, suppressed by powers of the Planck scale, M_{Pl} [15]. With the given particle content, we have two operators of mass-dimension five contributing to the down-quark and charged-lepton masses [15],

$$\mathsf{Y}_{\sigma 1}^{ij}\, 10_i^{ab}\, \overline{5}_{ja}\, \frac{\Sigma_b^c}{M_{\mathrm{Pl}}}\, \overline{H}_c + \mathsf{Y}_{\sigma 2}^{ij}\, 10_i^{ab}\, \overline{5}_{jc}\, \frac{\Sigma_b^c}{M_{\mathrm{Pl}}}\, \overline{H}_a \;. \tag{3}$$

The vacuum expectation value (vev) of Σ is proportional to hypercharge, $\langle\Sigma\rangle = \sigma\, \mathrm{diag}\,(2,2,2;-3,-3)$. Hence, the second operator modifies the relation (2),

$$\mathsf{Y}_d = \mathsf{Y}_e^\top + 5\frac{\sigma}{M_{\mathrm{Pl}}}\, \mathsf{Y}_{\sigma 2} \;. \tag{4}$$

Now we cannot diagonalize both Yukawa matrices simultaneously anymore. In the basis where the charged leptons are diagonal, we obtain

$$L_d\, \mathsf{D}_d R_d^\dagger = \mathsf{D}_e + 5\frac{\sigma}{M_{\mathrm{Pl}}}\, \widetilde{\mathsf{Y}}_{\sigma 2} \;; \tag{5}$$

D_i denote the diagonal Yukawa matrices, and L_d and R_d are unitary rotation matrices for the down-quark fields. The good agreement of the bottom and tau masses at the GUT scale indicates that the rotation matrices L_d and R_d have a non-trivial 1-2 block only,[5]

$$L_d,\, R_d \sim \begin{pmatrix} * & * & 0 \\ * & * & 0 \\ 0 & 0 & 1 \end{pmatrix} . \tag{6}$$

[4] The unification of down-quark and charged-lepton masses is a prediction of the SU(4) symmetry, which is present in the Pati-Salam model and respected in minimal SU(5).

[5] Even if $\mathsf{Y}_{\sigma 2}^{33} \sim 1$, it is suppressed with respect to Y_2^{33} by σ/M_{Pl}.

Hence, the effect of the additional rotations may only be seen in observables involving the first and second generations.

The effect of the dimension-five operators on proton decay has been studied in great detail [16]. In this paper, we point out that the rotation matrices L_d and R_d can be severely constrained by the precise measurements in K and B_d physics. This, in turn, allows for a complementary study of these operators and thus enables us to probe grand-unified models.

In the following, we will omit the indices of the higher-dimensional operators. For instance, we will denote the operators in Eq. (3)

$$\mathsf{Y}_\sigma^{ij}\, 10_i\, \overline{5}_j\, \frac{\Sigma}{M_{\rm Pl}}\, \overline{H} \equiv \mathsf{Y}_{\sigma 1}^{ij}\, 10_i^{ab}\, \overline{5}_{ja}\, \frac{\Sigma_b^c}{M_{\rm Pl}}\, \overline{H}_c + \mathsf{Y}_{\sigma 2}^{ij}\, 10_i^{ab}\, \overline{5}_{jc}\, \frac{\Sigma_b^c}{M_{\rm Pl}}\, \overline{H}_a \ . \tag{7}$$

Note that these index-less operators represent all possible combinations for the fields to form a singlet, and so Y_σ is an *effective* coupling matrix.

3 Framework

Let us now turn to SO(10) and consider a model proposed by Chang, Masiero, and Murayama (CMM) [9]. Here the matter fields are unified in the spinor representations, 16_i, together with the right-handed neutrinos. SO(10) is broken to SU(5) by a pair of Higgs spinors, $16_H + \overline{16}_H$. Next, an adjoint field, 45_H, breaks SU(5) and the electroweak symmetry is eventually broken by a pair of fundamental Higgs fields, 10_H and $10'_H$. In fact, both the SU(5) adjoint and the SU(5) singlet of 45_H acquire vevs, the latter (denoted by $v_0 \sim 10^{17}\,\text{GeV}$) being an order of magnitude larger than the former ($\sigma \sim 10^{16}\,\text{GeV}$).

The Yukawa couplings in the CMM superpotential read

$$W_Y = 16_i\, \mathsf{Y}_1^{ij}\, 16_j\, 10_H + 16_i\, \mathsf{Y}_2^{ij}\, 16_j\, \frac{45_H\, 10'_H}{M_{\rm Pl}} + 16_i\, \mathsf{Y}_N^{ij}\, 16_j \frac{\overline{16}_H \overline{16}_H}{M_{\rm Pl}} \ . \tag{8}$$

Let us discuss the individual terms in detail. In the fundamental Higgs field 10_H, only the up-type Higgs doublet H_u acquires a weak-scale vev such that the first term gives masses to the up quarks and neutrinos only. The masses for the down quarks and charged leptons are then generated through the vev of the down-type Higgs doublet H_d in the second fundamental Higgs field $10'_H$. (A second Higgs field with Yukawa couplings to the SM fermions is generally needed in order to have a non-trivial flavor structure.) They are obtained from the second term in Eq. (8) which is of mass-dimension five, in contrast to minimal SU(5). As indicated above, this operator actually stands for various, inequivalent effective operators with both the SU(5)-singlet and the SU(5)-adjoint vevs of the adjoint Higgs field 45_H such that the coupling matrix Y_2 can only be understood symbolically. The magnitude of this second mass term is determined by the vev of the SU(5)-singlet component, v_0, which contributes equally to down-quark and charged-lepton masses. The strong hierarchy between the t and b, τ masses then follows from the $v_0/M_{\rm Pl}$ suppression factor. The smaller SU(5)-breaking vev (σ), which is proportional to hypercharge as in SU(5), will be important for the modification of the light generation Yukawa couplings. The second term in Eq. (8) can be constructed in various ways, for example by integrating out SO(10) fields at the Planck scale. The corresponding couplings can be symmetric or antisymmetric [17], resulting in an asymmetric effective coupling matrix Y_2, as opposed to the symmetric matrices Y_1 and Y_N. Finally, the third term in Eq. (8), again a higher-dimensional operator, generates Majorana masses for the right-handed neutrinos.

We can always choose a basis where one of the Yukawa matrices in Eq. (8) is diagonal. In particular, the basis where Y_1^{ij} is diagonal will be referred to as the up-basis. In the CMM model, however, one

assumes that Y_1^{ij} and Y_N^{ij} are simultaneously diagonalizable. This assumption is motivated by the observed values for the fermion masses and mixings and might be a result of family symmetries. First, we note that the up quarks have a stronger hierarchy than the down quarks, charged leptons, and neutrinos. Consequently, the eigenvalues of Y_N must almost have a double hierarchy compared to Y_1. Then, given the Yukawa couplings in an arbitrary basis, we expect smaller off-diagonal entries in the rotation matrices of Y_1 and Y_N than in Y_2 because hierarchical masses generically correspond to small mixing. Moreover, the light neutrino mass matrix implies that, barring cancellations, the rotations needed to diagonalize Y_1 should be smaller than those in $V_{\rm CKM}$ [18]. Thus, even if Y_N is not exactly diagonal in the up-basis, the off-diagonal entries in its rotation matrix will be much smaller than the entries in $V_{\rm CKM}$ so that they cannot spoil the large mixings among d_R quarks generated by $V_{\rm PMNS}$.

Now, with Y_1 and Y_N being simultaneously diagonal, the flavor structure is (apart from supersymmetry-breaking terms, which we will discuss below) fully contained in the remaining coupling, Y_2. Let us assume for the moment that the relation (2) is valid. Then we can rewrite the superpotential in the SU(5) basis as

$$W_Y = 16_i\, \mathsf{D}_1^{ij}\, 16_j\, 10_H + 16_i \left(V_q^* \mathsf{D}_2 V_\ell\right)^{ij}\, 16_j\, \frac{45_H\, 10'_H}{M_{\rm Pl}} + 16_i\, \mathsf{D}_N^{ij}\, 16_j \frac{\overline{16}_H \overline{16}_H}{M_{\rm Pl}}\ , \tag{9}$$

where the second coupling is to be understood as $(Q, e^c)^\top\, V_q^* \mathsf{D}_2 V_\ell\, (d^c, L)\, 45_H 10'_H/M_{\rm Pl}$ (cf. Sec. 2). Then V_q and V_ℓ coincide with the quark and lepton mixing matrices, $V_{\rm CKM}$ and $V_{\rm PMNS}$, up to phases.[6] Note that the mass matrices of both down quarks and charged leptons have a lopsided structure.

As discussed in the previous section, the relation (2) needs to be modified. Using the SU(5)-breaking vev of 45_H, σ, we obtain

$$\mathsf{Y}_d = \mathsf{Y}_e^\top + 5\frac{\sigma}{v_0}\mathsf{Y}_\sigma\ , \tag{10}$$

in accordance with SU(5) discussed above. Again, this notation is symbolic, as Y_σ stems from several distinct operators. Without these corrections, the large atmospheric mixing angle could directly be translated to maximal mixing between the right-handed down squarks $\tilde{b}_R$ and $\tilde{s}_R$. Now the CKM matrix diagonalizes $\mathsf{Y}_d \mathsf{Y}_d^\dagger$ whereas the PMNS matrix diagonalizes $\mathsf{Y}_e \mathsf{Y}_e^\dagger$, such that we cannot give a general relation between the contributions of the correction operators and additional rotations. Let us therefore make the ansatz

$$R_d = (U\, V_\ell)^\top\ , \tag{11}$$

i.e., the rotation of the down-quark singlet fields differs from that of the lepton doublets by a unitary matrix U. Clearly, in absence of the correction operators, $U = \mathbb{1}$. As said before, the goal of this paper is to study how much the rotations parameterized by R_d differ from those of the charged leptons, i.e. whether a sizeable admixture of $\tilde{d}_R$ in $\tilde{s}'_R$ is allowed.

As discussed above, the good bottom-tau unification implies that the (33)-entry of U should be close to one, up to a phase, and the remaining entries of the third row and column should be small. Thus we parameterize U as

$$U = \begin{pmatrix} U_{11} & U_{12} & 0 \\ U_{21} & U_{22} & 0 \\ 0 & 0 & e^{i\phi_4} \end{pmatrix} = \begin{pmatrix} \cos\theta\, e^{i\phi_1} & -\sin\theta\, e^{i(\phi_1-\phi_2+\phi_3)} & 0 \\ \sin\theta\, e^{i\phi_2} & \cos\theta\, e^{i\phi_3} & 0 \\ 0 & 0 & e^{i\phi_4} \end{pmatrix}, \tag{12}$$

[6] In the up-basis, $V_{\rm CKM}$ is conventionally defined as the matrix that rotates the left-handed down-quark mass eigenstates into the weak eigenbasis, while the inverse of $V_{\rm PMNS}$ rotates the corresponding charged leptons. The transposition between R_d and V_ℓ in Eq. (11) is due to relation (2).

with $\theta \in [0, \pi/2]$. For concreteness, let us assume the tribimaximal form for the leptonic mixing matrix, corresponding to the mixing angles $\theta_{12} = \arcsin\left(1/\sqrt{3}\right) \simeq 35^\circ$, $\theta_{13} = 0^\circ$, and $\theta_{23} = 45^\circ$. In the up-basis, we can have V_q in its standard parametrization and thereby absorb five of the six phases. Then we can indeed identify $V_q = V_{\rm CKM}$. We cannot do so for V_ℓ since we would only move the phases from the down-quark Yukawa matrix to the down-squark soft-breaking masses. We therefore choose to have V_ℓ with six phases; to see them explicitly, let us write down the mixing matrix for $\theta_{13} \neq 0$,

$$V_\ell = \begin{pmatrix} \sqrt{\frac{2}{3}} c_{13}\, e^{i\alpha_1} & \frac{1}{\sqrt{3}} c_{13}\, e^{i\alpha_2} & s_{13}\, e^{i(\delta+\alpha_3)} \\ e^{i\alpha_4}\left(-\frac{1}{\sqrt{6}} - \frac{1}{\sqrt{3}} s_{13}\, e^{-i\delta}\right) & e^{i(-\alpha_1+\alpha_2+\alpha_4)}\left(\frac{1}{\sqrt{3}} - \frac{1}{\sqrt{6}} s_{13}\, e^{-i\delta}\right) & \frac{1}{\sqrt{2}} c_{13}\, e^{i(-\alpha_1+\alpha_3+\alpha_4)} \\ e^{i\alpha_5}\left(\frac{1}{\sqrt{6}} - \frac{1}{\sqrt{3}} s_{13}\, e^{-i\delta}\right) & e^{i(-\alpha_1+\alpha_2+\alpha_5)}\left(-\frac{1}{\sqrt{3}} - \frac{1}{\sqrt{6}} s_{13}\, e^{-i\delta}\right) & \frac{1}{\sqrt{2}} c_{13}\, e^{i(-\alpha_1+\alpha_3+\alpha_5)} \end{pmatrix}, \tag{13}$$

where $c_{13} = \cos\theta_{13}$ and $s_{13} = \sin\theta_{13}$. In this parametrization, we can easily identify the standard phase, δ, and then the standard form for $V_{\rm PMNS}$ is given by $V_{\rm PMNS} = P_L V_\ell P_R$, where

$$P_L = {\rm diag}\left(e^{-i\alpha_1},\, e^{-i\alpha_4},\, e^{-i\alpha_5}\right), \qquad\qquad P_R = {\rm diag}\left(1,\, e^{i(\alpha_1-\alpha_2)},\, e^{i(\alpha_1-\alpha_3)}\right). \tag{14}$$

If θ_{13} is indeed zero, the phase δ drops out of the matrix (13). This situation is familiar from the standard model: CP violation requires $\theta_{13} \neq 0$. Altogether, for $\theta_{13} = 0$, the mixing matrix for the right-handed down quarks in Eq. (11) reads

$$R_d = \frac{1}{\sqrt{6}} \begin{pmatrix} 2U_{11}\, e^{i\alpha_1} - U_{12}\, e^{i\alpha_4} & 2U_{21}\, e^{i\alpha_1} - U_{22}\, e^{i\alpha_4} & e^{i(\phi_4+\alpha_5)} \\ \sqrt{2}\, e^{i\alpha_2}\left(U_{11} + U_{12}\, e^{i(\alpha_4-\alpha_1)}\right) & \sqrt{2}\, e^{i\alpha_2}\left(U_{21} + U_{22}\, e^{i(\alpha_4-\alpha_1)}\right) & -\sqrt{2}\, e^{i(\phi_4-\alpha_1+\alpha_2+\alpha_5)} \\ \sqrt{3} U_{12}\, e^{i(-\alpha_1+\alpha_3+\alpha_4)} & \sqrt{3} U_{22}\, e^{i(-\alpha_1+\alpha_3+\alpha_4)} & \sqrt{3}\, e^{i(\phi_4-\alpha_1+\alpha_3+\alpha_5)} \end{pmatrix} \tag{15}$$

with U_{ij} as given in Eq. (12).

Due to the absence of right-handed multiplets in the standard model, mixing among the right-handed down quarks is unobservable. With supersymmetry, however, the mixing of the corresponding squarks potentially leads to enhanced amplitudes for flavor-changing processes. As mentioned in the Introduction, we will assume universal soft masses at the Planck scale. This universality, however, is no longer present at the electroweak scale. For the scalar masses, this is due to the large Yukawa coupling of the third generation in the renormalization group evolution (RGE), such that

$$\mathsf{M}^2_{\tilde{d}}(M_Z) = {\rm diag}\left(m^2_{\tilde{d}},\; m^2_{\tilde{d}},\; m^2_{\tilde{d}}\left(1 - \Delta_{\tilde{d}}\right)\right) \tag{16}$$

in the case of the $\tilde{d}_R$ soft-breaking terms. The fast RGE between $M_{\rm Pl}$ and v_0 allows for rather large values of $\Delta_{\tilde{d}}$ [9, 11]. Now choosing the super-CKM basis where the down quarks are mass eigenstates, this matrix is no longer diagonal; in particular, all elements of the 2-3 block are of comparable size:

$$\widetilde{\mathsf{M}}^2_{\tilde{d}} = R_d^\dagger\, \mathsf{M}^2_{\tilde{d}}\, R_d = m^2_{\tilde{d}} \begin{pmatrix} 1 - \sin^2\theta\, \Delta_{\tilde{d}}/2 & \sin(2\theta)\, e^{-i\phi_K}\, \Delta_{\tilde{d}}/4 & \sin\theta\, e^{-i\phi_{B_d}}\, \Delta_{\tilde{d}}/2 \\ \sin(2\theta)\, e^{i\phi_K}\, \Delta_{\tilde{d}}/4 & 1 - \cos^2\theta\, \Delta_{\tilde{d}}/2 & -\cos\theta\, e^{-i\phi_{B_s}}\, \Delta_{\tilde{d}}/2 \\ \sin\theta\, e^{i\phi_{B_d}}\, \Delta_{\tilde{d}}/2 & -\cos\theta\, e^{i\phi_{B_s}}\, \Delta_{\tilde{d}}/2 & 1 - \Delta_{\tilde{d}}/2 \end{pmatrix}, \tag{17}$$

$$\phi_K = \phi_1 - \phi_2\ , \qquad \phi_{B_s} = \phi_3 - \phi_4 + \alpha_4 - \alpha_5\ , \qquad \phi_{B_d} = \phi_1 - \phi_2 + \phi_3 - \phi_4 + \alpha_4 - \alpha_5\ .$$

This observation motivated detailed studies of $b \to s$ transitions in supersymmetric GUT models, in particular the decay $b \to s\gamma$ and $B_s - \overline{B_s}$ mixing [9, 10, 11]. In the following, we will study the impact of the 1-2 and 1-3 blocks, generated by the angle θ in Eq. (12), on the analogous $s \to d$ and $b \to d$ transitions, focussing on $K - \overline{K}$ and $B_d - \overline{B_d}$ mixing.

4 Meson-Antimeson Mixing

The oscillations of a $P^0 - \overline{P^0}$ meson system can be described by a Schrödinger-type equation,

$$i\frac{d}{dt}\begin{pmatrix}|P^0(t)\rangle\\ |\overline{P^0}(t)\rangle\end{pmatrix} = \left[M^P - \frac{i}{2}\Gamma^P\right]\begin{pmatrix}|P^0(t)\rangle\\ |\overline{P^0}(t)\rangle\end{pmatrix}, \tag{18}$$

where M^P and Γ^P are two 2×2 hermitian matrices which encode the four transitions $P^0/\overline{P^0} \to P^0/\overline{P^0}$ via virtual and physical intermediate states, respectively. The physical states $|P_1^0\rangle$ and $|P_2^0\rangle$ are obtained by diagonalizing $M^P - \frac{i}{2}\Gamma^P$. The relevant quantity to study new-physics effects in $P^0 - \overline{P^0}$ mixing is the local contribution to the off-diagonal element of M^P:

$$M_{12}^P = \frac{1}{2M_P}\left\langle P^0\middle|\mathcal{H}_{\rm eff}^{\Delta F=2}\middle|\overline{P^0}\right\rangle, \tag{19}$$

with M_P, the average meson mass $(M_{P_1} + M_{P_2})/2$. The effective Hamiltonian $\mathcal{H}_{\rm eff}^{\Delta F=2}$, which comprises in general eight effective operators,

$$\mathcal{H}_{\rm eff}^{\Delta F=2} = \frac{G_F^2 M_W^2}{16\pi^2}\sum_{i=1}^{8} C_P^i(\mu_P)\, Q_P^i(\mu_P), \tag{20}$$

is conveniently expressed at the scale $\mu_P \sim M_P$ in the B_d and B_s systems, and at the scale $\mu_P \lesssim m_c$ in the kaon system. For an extensive introduction into the formalism of $K - \overline{K}$ and $B_{d,s} - \overline{B}_{d,s}$ mixing, see e.g. Ref. [19].

One observable which is particularly well-suited to constrain the additional rotation of the $\tilde{d}_R$ and $\tilde{s}_R$ squarks in Eq. (12) is

$$|\epsilon_K| = \kappa_\epsilon \frac{\mathrm{Im}\left(M_{12}^K\right)}{\sqrt{2}\Delta M_K}, \tag{21}$$

which measures the amount of CP-violation in $K - \overline{K}$ mixing amplitudes. Indeed, $|\epsilon_K|$ is very small in the standard model and its experimental value, measured with high precision, leaves only little room for new physics. The correction factor κ_ϵ above parameterizes both the small deviation of $\sin\phi_{\epsilon_K} = \Delta M_K/(\Delta M_K^2 + \Delta\Gamma_K^2/4)^{1/2}$ from $1/\sqrt{2}$ and the small contribution from the phase of the isospin-zero $K \to \pi\pi$ decay amplitude. This factor was estimated to $\kappa_\epsilon = 0.92 \pm 0.02$ [20] assuming the standard model. Its modification in the presence of new physics will not alter our analysis, and we will ignore this complication. The mass difference ΔM_K between the two eigenstates K_L and K_S receives both short-distance and long-distance contributions, such that the constraint on possible new-physics effects in the short-distance part,

$$(\Delta M_K)^{\rm SD} = 2\,\mathrm{Re}\left(M_{12}^K\right), \tag{22}$$

is somewhat diluted among hadronic uncertainties. Despite its precise experimental knowledge, ΔM_K will thus play a minor role in our study.

On the contrary, when new sources of CP-violation in the kaon system are small, two observables in the B_d system will prove useful to gain information on the mixing angle θ. These are the mass difference,

$$\Delta M_d = 2\left|M_{12}^{B_d}\right|, \tag{23}$$

$\Delta M_K^{\rm exp} = (3.483 \pm 0.006) \cdot 10^{-12}\,{\rm MeV}$ [22]	$\lvert\epsilon_K\rvert^{\rm exp} = (2.229 \pm 0.012) \cdot 10^{-3}$ [22]
$\Delta M_d^{\rm exp} = (3.337 \pm 0.033) \cdot 10^{-10}\,{\rm MeV}$ [22]	$S_{J/\psi K_S}^{\rm exp} = 0.671 \pm 0.024$ [23]
$\Delta M_s^{\rm exp} = (117.0 \pm 0.8) \cdot 10^{-10}\,{\rm MeV}$ [22]	$\phi_s^{\rm exp} = (-0.77\,^{+0.29}_{-0.37}) \cup (-2.36\,^{+0.37}_{-0.29})\,{\rm rad}$ [23]

Table 1: Current experimental values of the various $\Delta F = 2$ observables considered in Eqs. (21-26).

and the coefficient of the $\sin(\Delta M_d\, t)$ term in the $B_d \to J/\psi K_S$ time-dependent CP asymmetry,

$$S_{J/\psi K_S} = \sin\left(2\beta + \phi_d^\Delta\right) \simeq {\rm Im}\left(\frac{M_{12}^{B_d}}{\left|M_{12}^{B_d}\right|}\right), \quad \beta \equiv \arg\left[-\frac{V_{td}^* V_{tb}}{V_{cd}^* V_{cb}}\right], \quad \phi_d^\Delta \equiv \arg\frac{M_{12}^{B_d}}{M_{12}^{B_d,\,\rm SM}}. \tag{24}$$

The phase ϕ_d^Δ parameterizes CP-violating effects beyond the SM in $B_d - \overline{B_d}$ mixing. Here and in the following, we use the standard CKM phase convention.

Finally, we will also consider the mass difference in the B_s system,

$$\Delta M_s = 2\left|M_{12}^{B_s}\right|, \tag{25}$$

as well as the phase measured in the $B_s \to J/\psi\,\phi$ time-dependent angular distribution,

$$-2\beta_s^{\rm eff} = -2\beta_s + \phi_s^\Delta \simeq \arcsin\left({\rm Im}\,\frac{M_{12}^{B_s}}{\left|M_{12}^{B_s}\right|}\right), \quad \beta_s \equiv -\arg\left[-\frac{V_{ts}^* V_{tb}}{V_{cs}^* V_{cb}}\right], \quad \phi_s^\Delta \equiv \arg\frac{M_{12}^{B_s}}{M_{12}^{B_s,\,\rm SM}}. \tag{26}$$

In the SM, β_s is tiny: $2\beta_s \simeq 0.04$. As long as ϕ_s^Δ is not too small, we thus have $-2\beta_s^{\rm eff} \simeq \phi_s^\Delta$. On the other hand, one also has $\phi_s \equiv \arg(-M_{12}^{B_s}/\Gamma_{12}^{B_s}) \simeq \phi_s^\Delta$ [21]. In the following, we will thus identify $\phi_s = -2\beta_s^{\rm eff}$.

The current experimental values of the various observables above are reported in Tab. 1.

4.1 Standard-Model Contributions

In the standard model, W box diagrams with virtual t and/or c flavors generate the effective operators

$$Q_K^{\rm VLL} = \left(\overline{d}_L \gamma_\mu s_L\right)\left(\overline{d}_L \gamma^\mu s_L\right), \qquad Q_{B_q}^{\rm VLL} = \left(\overline{q}_L \gamma_\mu b_L\right)\left(\overline{q}_L \gamma^\mu b_L\right) \tag{27}$$

for kaons (see Fig. 1(a)) and B_q ($q = s$ or d), respectively. The corresponding Wilson coefficients at the scale μ_P read

$$\begin{aligned} C_K^{\rm VLL}(\mu_K) &= 4U_K(\mu_K)\left[(V_{cd}^* V_{cs})^2 \eta_1 S_0(x_c) + 2(V_{cd}^* V_{cs})(V_{td}^* V_{ts})\eta_3 S_0(x_c, x_t) + (V_{td}^* V_{ts})^2\,\eta_2 S_0(x_t)\right], \\ C_{B_q}^{\rm VLL}(\mu_{B_q}) &= 4U_{B_q}(\mu_{B_q})(V_{tq}^* V_{tb})^2 \eta_B S_0(x_t), \end{aligned} \tag{28}$$

where the factors

$$U_K(\mu) = \left[\alpha_s^{(3)}(\mu)\right]^{-2/9}\left[1 + \frac{\alpha_s^{(3)}(\mu)}{4\pi} J_3\right] \quad \text{and} \quad U_{B_q}(\mu) = \left[\alpha_s^{(5)}(\mu)\right]^{-6/23}\left[1 + \frac{\alpha_s^{(5)}(\mu)}{4\pi} J_5\right] \tag{29}$$

encode the μ_K, μ_{B_q}-dependent parts of the short-distance QCD corrections up to next-to-leading order (NLO), while η_i account for their μ_K, μ_{B_q}-independent contributions [24, 25]; their values are given in Tab. 2. The loop functions $S_0(x_q)$ and $S_0(x_c, x_t)$ are listed in the appendix. Finally, $x_q = m_q^2/M_W^2$ and $m_q \equiv \overline{m}_q(m_q)$ is the $\overline{\rm MS}$ mass.

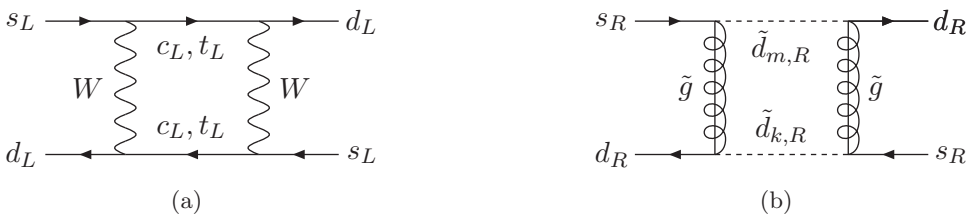

Figure 1: Dominant short-distance contributions to M_{12}^K (a) in the SM; (b) in the CMM extension.

In order to compute M_{12}^{K,B_q}, we still need the matrix elements of $Q_K^{\rm VLL}$ and $Q_{B_q}^{\rm VLL}$. These are parameterized in terms of "bag factors" B_P, computed at the scale $\mu = \mathcal{O}(\mu_P)$:

$$\left\langle P^0 \middle| Q_P^{\rm VLL}(\mu) \middle| \overline{P^0} \right\rangle = \frac{2}{3} M_P^2 F_P^2 B_P(\mu), \tag{30}$$

where F_P is the decay constant of the P meson. The scale dependences of $U_P(\mu)$ and $B_P(\mu)$ cancel each other, so that it is convenient to define the renormalization-group-invariant parameters $\widehat{B}_P = B_P(\mu)U_P(\mu)$. Eqs. (28), (29), and (30) then lead to

$$\begin{aligned}
(M_{12}^K)^{\rm SM} &= \frac{G_F^2 M_W^2}{12\pi^2} M_K F_K^2 \widehat{B}_K \left[(\lambda_{ds}^c)^2 \eta_1 S_0(x_c) + 2(\lambda_{ds}^c)(\lambda_{ds}^t)\eta_3 S_0(x_c, x_t) + (\lambda_{ds}^t)^2 \eta_2 S_0(x_t) \right], \\
(M_{12}^{B_q})^{\rm SM} &= \frac{G_F^2 M_W^2}{12\pi^2} M_{B_q} F_{B_q}^2 \widehat{B}_{B_q} (\lambda_{qb}^t)^2 \eta_B S_0(x_t),
\end{aligned} \tag{31}$$

where one defines $\lambda_{ij}^k = V_{ki}^* V_{kj}$.

4.2 CMM Contributions

In the context of the CMM model, the dominant supersymmetric effects originate from gluino box diagrams with virtual $\tilde{d}_R$, $\tilde{s}_R$, and $\tilde{b}_R$ flavors due to the large mixings in Eq. (15). This gives rise to the parity-reflected operators (Fig. 1(b))

$$Q_K^{\rm VRR} = \left(\overline{d}_R \gamma_\mu s_R\right) \left(\overline{d}_R \gamma^\mu s_R\right), \qquad Q_{B_q}^{\rm VRR} = \left(\overline{q}_R \gamma_\mu b_R\right) \left(\overline{q}_R \gamma^\mu b_R\right). \tag{32}$$

The initial conditions for the Wilson coefficients at the SUSY scale $M_S = \mathcal{O}(m_{\tilde{d}_j}, m_{\tilde{g}})$ read [9, 11]

$$C_{K,B_q}^{\rm CMM}(M_S) = \frac{16\pi^2}{G_F^2 M_W^2} \frac{\alpha_s^2(M_S)}{2m_{\tilde{g}}^2} \sum_{k,m=1}^{3} (R_d)_{mj} (R_d)_{mi}^* (R_d)_{kj} (R_d)_{ki}^* \, L_0(r_m, r_k), \tag{33}$$

where $(i,j) = (1,2)$ in the kaon case, $(1,3)$ in the B_d case, and $(2,3)$ in the B_s case. The loop function $L_0(r_m, r_k)$ is defined in the appendix, the down-type squark mixing matrix R_d was given in Eq. (15), and $r_j = m_{\tilde{d}_j}^2/m_{\tilde{g}}^2$. Exploiting the mass degeneracy of the first two generations (see Eq. (16)) as well as the unitarity of R_d, Eq. (33) simplifies to

$$C_{K,B_q}^{\rm CMM}(M_S) = \frac{16\pi^2}{G_F^2 M_W^2} \frac{\alpha_s^2(M_S)}{2m_{\tilde{g}}^2} \left[(R_d)_{3j} (R_d)_{3i}^* \right]^2 \left\{ L_0(r_1, r_1) - 2L_0(r_1, r_3) + L_0(r_3, r_3) \right\}, \tag{34}$$

$$r_1 = m_{\tilde{d}}^2/m_{\tilde{g}}^2, \qquad r_3 = m_{\tilde{d}}^2 \left(1 - \Delta_{\tilde{d}}\right)/m_{\tilde{g}}^2. \tag{35}$$

The RGE of the above Wilson coefficients from the scale M_S down to the scale μ_{K,B_q} is performed in two steps: first, the leading-order matching coefficients in Eq. (34) are evolved down to $\mu_t = \mathcal{O}(m_t)$ by means of the leading-order RGE factor $\eta_6 = [\alpha_s^{(6)}(M_S)/\alpha_s^{(6)}(\mu_t)]^{2/7}$. The remaining evolution, running

over two orders of magnitude, is achieved using NLO formulas – essentially the $U_K(\mu_K)$, η_2, $U_{B_q}(\mu_{B_q})$, and η_B factors of Sec. 4.1. The $\mathcal{O}(\alpha_s)$ QCD corrections to the SM function $S_0(x_t)$ at the scale μ_t, which are contained in η_2 and η_B, should be removed. Denoting them by $r = 0.985$ [25], we get

$$C_K^{\rm CMM}(\mu_K) = U_K(\mu_K)\,\eta_2\,\frac{1}{r}\,\eta_6\,C_K^{\rm CMM}(M_S), \tag{36}$$

and similarly for $C_{B_q}^{\rm CMM}(\mu_{B_q})$. The cancellation of the μ_t-dependence between the two parts of the evolution is of course incomplete, yet this is a numerically small effect which can be neglected.

The bag parameters of the effective operators $Q_K^{\rm VRR}$ and $Q_{B_q}^{\rm VRR}$ are identical to those of the SM operators in Eq. (30) such that the CMM contributions to the matrix elements M_{12}^P finally read

$$\begin{aligned}
(M_{12}^K)^{\rm CMM} &= \frac{\alpha_s^2(M_S)}{6m_{\tilde g}^2} M_K F_K^2 \widehat{B}_K\,\frac{e^{-2i\phi_K}\sin^2(2\theta)}{16}\,\frac{\eta_2\eta_6}{r}\,S^{(\tilde g)}(r_1,r_3),\\
(M_{12}^{B_d})^{\rm CMM} &= \frac{\alpha_s^2(M_S)}{6m_{\tilde g}^2} M_{B_d} F_{B_d}^2 \widehat{B}_{B_d}\,\frac{e^{-2i\phi_{B_d}}\sin^2\theta}{4}\,\frac{\eta_B\eta_6}{r}\,S^{(\tilde g)}(r_1,r_3),\\
(M_{12}^{B_s})^{\rm CMM} &= \frac{\alpha_s^2(M_S)}{6m_{\tilde g}^2} M_{B_s} F_{B_s}^2 \widehat{B}_{B_s}\,\frac{e^{-2i\phi_{B_s}}\cos^2\theta}{4}\,\frac{\eta_B\eta_6}{r}\,S^{(\tilde g)}(r_1,r_3),
\end{aligned} \tag{37}$$

where we explicitly display the factors $(R_d)_{3i}$ in Eq. (34), $S^{(\tilde g)}(r_1,r_3) = L_0(r_1,r_1) - 2L_0(r_1,r_3) + L_0(r_3,r_3)$, and the CMM phases ϕ_K, ϕ_{B_d}, and ϕ_{B_s} have been defined in Eq. (17). Note that they fulfill the relation $\phi_{B_d} = \phi_K + \phi_{B_s}$.

4.3 Additional Supersymmetric Contributions

Finally, we comment on the supersymmetric contributions which do not exhibit the large enhancement factors characteristic of the CMM model, namely charged-Higgs(H)-quark and chargino(χ)-squark box diagrams. They do not introduce new operators, and the flavor structure of the corresponding matrix elements is the same as in the SM,

$$\begin{aligned}
(M_{12}^K)^{H+\chi} &= \frac{G_F^2 M_W^2}{12\pi^2} M_K F_K^2 \widehat{B}_K \left\{2(\lambda_{ds}^c)(\lambda_{ds}^t)\eta_3^H S_H(c,t) + (\lambda_{ds}^t)^2\,\eta_2\,[S_H(t,t) + S_\chi(t,t)]\right\},\\
(M_{12}^{B_q})^{H+\chi} &= \frac{G_F^2 M_W^2}{12\pi^2} M_{B_q} F_{B_q}^2 \widehat{B}_{B_q} (\lambda_{qb}^t)^2 \eta_B\,[S_H(t,t) + S_\chi(t,t)]\,.
\end{aligned} \tag{38}$$

The loop functions $S_H(c,t)$, $S_H(t,t)$, and $S_\chi(t,t)$ are given explicitly in Ref. [7]. The factor $\eta_3^H = 0.21$ [7] denotes leading-order QCD corrections to the charged-Higgs box with virtual flavors (c,t). Numerically, charged-Higgs and chargino contributions are small compared to CMM effects. We checked explicitly that they can be neglected in our analysis.

5 Numerical Analysis

We are now ready to investigate the constraints of $K - \overline{K}$ and $B_d - \overline{B_d}$ mixing on the angle θ in the down-type squark mixing matrix R_d. Since we do not expect a miraculous cancellation of the phases ϕ_1 and ϕ_2, we will first focus on the case where $\sin 2\phi_K \sim \mathcal{O}(1)$ (Sec. 5.2) and derive constraints on θ from $|\epsilon_K|$ alone. We will then turn to the special case $\sin 2\phi_K \sim 0$ (Sec. 5.3) where, as we will see, interesting constraints can still be obtained from ΔM_K, ΔM_d, $S_{J/\psi K_S}$, and $\Delta M_d/\Delta M_s$.

The values of the various input parameters adopted in our numerical analysis are reported in Tab. 2. Inputs related to CKM elements have to be protected from new-physics impact. To this end, we

$\kappa_\epsilon = 0.92 \pm 0.02$	[20]	$\lvert V_{us}\rvert = 0.2246 \pm 0.0012$	[26]
$F_K = (156.1 \pm 0.8)$ MeV	[26]	$\lvert V_{cb}\rvert = (41.6 \pm 0.6) \cdot 10^{-3}$	[22]
$\widehat{B}_K = 0.75 \pm 0.07$	[27]	$\lvert V_{ub}\rvert = (3.95 \pm 0.35) \cdot 10^{-3}$	[22]
$F_{B_s}\widehat{B}^{1/2}_{B_s} = (270 \pm 30)$ MeV	[27]	$\gamma = (70.7^{+5.7}_{-7.0})^\circ$	[see text]
$\xi \equiv \frac{F_{B_s}\widehat{B}^{1/2}_{B_s}}{F_{B_d}\widehat{B}^{1/2}_{B_d}} = (1.21 \pm 0.04)$	[27]	$\eta_1 = (1.32 \pm 0.32)\left[\frac{1.30\,\text{GeV}}{\overline{m}_c(m_c)}\right]^{1.1}$	[24, 28]
$\overline{m}_c(m_c) = (1.266 \pm 0.014)$ GeV	[31]	$\eta_2 = 0.57 \pm 0.01$	[25, 28]
$\overline{m}_t(m_t) = (162.1 \pm 1.2)$ GeV	[32, 30]	$\eta_3 = 0.47 \pm 0.05$	[24, 28]
$\alpha_s(M_Z) = 0.1176 \pm 0.0020$	[22]	$\eta_B = 0.551 \pm 0.007$	[25, 29]

Table 2: Input parameters.

determine the CKM matrix from the elements $|V_{ub}|$, $|V_{cb}|$, $|V_{us}|$, and δ, the CP-phase in the standard parametrization, which equals the angle γ of the unitarity triangle to very good accuracy. The three CKM elements are extracted from tree-level decays. We use $|V_{us}| = 0.2246 \pm 0.0012$ [26], the inclusive determination $|V_{cb}| = (41.6 \pm 0.6) \cdot 10^{-3}$ [22], and the average of inclusive and exclusive determinations $|V_{ub}| = (3.95 \pm 0.35) \cdot 10^{-3}$ [22]. The angle γ is determined via $\gamma = \pi - \alpha - \beta = \pi - \alpha^{\text{eff}} - \beta^{\text{eff}}$, with $\beta^{\text{eff}} = \beta + \phi_d^\Delta/2 = (21.1 \pm 0.9)^\circ$ from $S_{J/\psi K_S}$ [23] and $\alpha^{\text{eff}} = \alpha - \phi_d^\Delta/2 = (88.2^{+6.1}_{-4.8})^\circ$ from $B \to \pi\pi,\ \pi\rho,\ \rho\rho$ decays [33]. The dependence on the new-physics phase ϕ_d^Δ cancels out in the sum $\alpha^{\text{eff}} + \beta^{\text{eff}}$, such that $\gamma = (70.7^{+5.7}_{-7.0})^\circ$ is indeed free from new-physics contamination.

No assumption is made on the squark mixing parameters θ, ϕ_K, ϕ_{B_d}, and ϕ_{B_s} prior to the analysis of the observables in Tab. 1. The supersymmetric parameters (in particular $m_{\tilde{g}}$, r_1, and r_3, or equivalently $m_{\tilde{g}}$, $m_{\tilde{d}}$, and $\Delta_{\tilde{d}}$), on the other hand, are chosen such as to satisfy the constraints coming from other observables. The identification of viable sets of SUSY parameters is the subject of the next section.

5.1 CMM Parameter Sets

In the CMM model, the large number of free SUSY parameters shrinks to six input parameters at the electroweak scale (in addition to θ and the CMM phases ϕ_K, ϕ_{B_d}, and ϕ_{B_s}). These can be chosen as the gluino mass $m_{\tilde{g}}$, the first-generation $\tilde{d}_R$ and $\tilde{u}_R$ soft masses $m_{\tilde{d}}$ and $m_{\tilde{u}}$[7], the ratio of the (11)-elements of the trilinear and Yukawa couplings $a_d^1 = (A_d)_{11}/(Y_d)_{11}$, the phase of the μ parameter in the Higgs potential $\arg(\mu)$, and the ratio of the two Higgs-doublet vevs $\tan\beta$. The RGE links these CMM inputs to the remaining SUSY parameters via the assumption of universal soft-breaking parameters at the Planck scale and the intermediate SO(10) and SU(5) GUT relations. Note that the similar input parameters in the CMM model and in specific SUSY scenarios without grand unification still lead to very different phenomenologies. In such well-studied scenarios as mSUGRA or the CMSSM, the SUSY-breaking parameters are universal at M_{GUT}, as mentioned in the Introduction, leaving the universal gaugino and scalar masses, $m_{1/2}$ and m_0, the trilinear coupling A, as well as the sign of μ and $\tan\beta$ as free parameters. In contrast to GUT models, however, these scenarios do not relate quarks and leptons to each other; the MSSM fields can be rotated independently and the large lepton mixing angles do not become visible in the quark sector.

To establish benchmarks for our analysis of the down-squark mixing angle θ in $K - \overline{K}$ and $B_d - \overline{B}_d$ mixing, we make sure that the chosen CMM input parameters are in accord with the other observables sensitive to CMM effects, and that they respect constraints common to generic SUSY scenarios. To this end, we make use of the *Mathematica* code written by the authors of Ref. [12], which implements the

[7]The specification of both $m_{\tilde{d}}$ and $m_{\tilde{u}}$ fixes the D-term scalar mass splitting [12, 34].

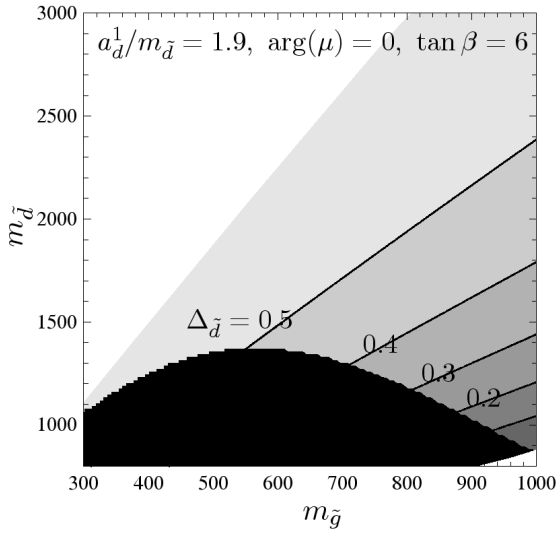

Figure 2: Down-squark mass splitting $\Delta_{\tilde{d}}$ as a function of $m_{\tilde{g}}$ and $m_{\tilde{d}}$ [GeV]. White: negative soft masses. Black: excluded by lower bound on light Higgs mass.

relations between the CMM input parameters discussed above and the remaining SUSY parameters at the electroweak scale. The most restrictive observable is the experimental lower bound on the mass of the lightest Higgs boson m_h. For small values of $\tan\beta$ it is close to the SM bound, $m_h \geq 114.4\,\text{GeV}$ [35]. The main radiative corrections to the tree-level Higgs mass in the MSSM, $m_h^{\text{tree}} \leq M_Z|\cos 2\beta|$, stem from (s)top loops. For very small values of $\tan\beta \approx 3$ the large top Yukawa coupling in the RGE drives the stop mass to low values, such that the Higgs mass bound cannot be fulfilled. In our analysis we choose $\tan\beta = 6$, such that the top Yukawa coupling gets smaller, but the natural hierarchy between the top and bottom Yukawa couplings, induced by v_0/M_{Pl} in the CMM superpotential, is preserved. We fix the inputs $a_d^1/m_{\tilde{d}} = 1.9$ and $\arg(\mu) = 0$, such that the allowed space for $m_{\tilde{g}}$ and $m_{\tilde{d}}$ around 1 TeV is large. Finally, we take $m_{\tilde{u}} = m_{\tilde{d}}$ as in Ref. [12]. In Fig. 2 we show the mass splitting parameter $\Delta_{\tilde{d}}$ in the $m_{\tilde{g}} - m_{\tilde{d}}$ plane for this scenario. Black regions are excluded by the Higgs mass bound. White regions are forbidden due to negative soft mass parameters. In summary, down-squark masses $m_{\tilde{d}} \leq 1\,\text{TeV}$ and gluino masses $m_{\tilde{g}} \leq 300\,\text{GeV}$ are not possible in the CMM model for $\tan\beta \leq 6$. As the light Higgs mass bound strongly cuts into the CMM parameter space, processes reflecting the large atmospheric neutrino mixing angle like $\tau \to \mu\gamma$ and $b \to s\gamma$ do not give additional constraints (or, vice versa, the light Higgs mass bound sets an upper limit on CMM effects in those observables). This also holds for ΔM_s, though in this case agreement with the data may require to restrict the range of ϕ_{B_s} values.

Based on these considerations, we select three sets of CMM input parameters, given in Tab. 3. As said above, these parameters are defined at the electroweak scale, more precisely at M_Z, in Ref. [12]. For consistency, we will thus set $M_S = M_Z$ (and correspondingly $\eta_6 = 1$, neglecting the small effect of $m_t \neq M_Z$) in our analysis of meson-antimeson mixing. As we will see, the analytic expressions in Eq. (37) essentially depend on $m_{\tilde{g}}$ and $\Delta_{\tilde{d}}$, with little sensitivity to the ratio $m_{\tilde{d}}/m_{\tilde{g}}$.

Sets 2 and 3 do satisfy the ΔM_s constraint for all values of θ and ϕ_{B_s}, while Set 1 requires $|2\phi_{B_s}|$ to be between 1.3 and 2.3 radians when $|\sin\theta| \lesssim 0.5$ to satisfy this constraint. Note that especially Set 1 (with small $m_{\tilde{g}}$ and large $\Delta_{\tilde{d}}$) is chosen such that CMM effects in $b \to s$, $b \to d$, and $s \to d$ transitions are large.

	$m_{\tilde{g}}$ [GeV]	$m_{\tilde{d}}$ [GeV]	$\Delta_{\tilde{d}}$	$\theta^{\max}$ [°]
Set 1	500	1500	0.55	0.5
Set 2	700	1500	0.46	0.8
Set 3	700	2000	0.54	0.7

Table 3: CMM parameter sets for fixed $a_d^1/m_{\tilde{d}} = 1.9$, $\arg(\mu) = 0$, and $\tan\beta = 6$, satisfying the constraints discussed in Sec. 5.1. The last column shows the maximal mixing angle $\theta^{\max}$ allowed by $|\epsilon_K|$ for $\sin 2\phi_K = 1$ (the symmetric solution $\theta \in [(\pi - \theta^{\max})/2, \pi/2]$ is excluded by B physics observables, see Fig. 4).

5.2 Scenario I: $\sin 2\phi_K \sim \mathcal{O}(1)$

As long as the CMM phase ϕ_K is not too close to zero, $|\epsilon_K|$ gives the best constraint on θ. The dependence of $\theta^{\max}$ on the relevant combinations of parameters, i.e., $\sin 2\phi_K/m_{\tilde{g}}^2$, $m_{\tilde{d}}/m_{\tilde{g}}$, and $\Delta_{\tilde{d}}$, is summarized in Fig. 3-left. The plain black and dashed gray lines correspond to Set 2 and Set 1, respectively, while the two other lines are obtained by interchanging $m_{\tilde{d}}/m_{\tilde{g}}$. As one can see, the dependence on $m_{\tilde{d}}/m_{\tilde{g}}$ is indeed quite mild. Typically, for $|\sin 2\phi_K|/m_{\tilde{g}}^2 \gtrsim 1\,\text{TeV}^{-2}$, $\theta^{\max}$ is of the order of one degree. Fig. 3 has been obtained treating the errors in Tab. 2 as flat, yet a different error treatment – and/or inflated errors in Tab. 2 – would not change this picture significantly. Fixing ϕ_K to $\pi/2$, the precise limits obtained for the various parameter sets defined in Sec. 5.1 are displayed in the last column of Tab. 3. The small contributions in Sec. 4.3 have no impact on these numbers.

In the B_d and B_s systems, the SM contributions are not as suppressed as for ϵ_K. Consequently, the smallness of $\theta^{\max}$ prevents any visible effect in ΔM_d and $S_{J/\psi K_S}$, while the formulas for ΔM_s and ϕ_s are well approximated setting $\theta = 0$. Interestingly, sizeable CMM contributions in the B_s system may be welcome to reduce the 2.2σ discrepancy between the SM prediction for ϕ_s and its experimental value [23]. Within Set 1 it is possible to bring this discrepancy down to the one-sigma level while satisfying all existing constraints, see Fig. 3-right.

Finally, we briefly comment on the dependence of $\theta^{\max}$ on the hypothesis of tribimaximal lepton mixing. In particular, one might expect the 23-mixing angle to be large but not $\pi/4$. In this case, $\text{Im}\left[(R_d)_{32}(R_d)_{31}^*\right]^2 = -\frac{1}{4}\sin^4\theta_{23}\sin^2(2\theta)\sin(2\phi_K)$ for $\theta_{13} = 0$. Hence, for large θ_{23}, the constraints on θ do not differ much. For a sizeable 13-mixing angle in V_ℓ, $|\epsilon_K|$ gets additional contributions:

$$\begin{aligned}\Delta\left(\text{Im}\left[(R_d)_{32}(R_d)_{31}^*\right]^2\right) = \sin\theta_{13}\,\sin^3\theta_{23}\,\sin(2\theta)\,[&\sin(2\phi_K)\cos(2\theta)\cos(\phi_3-\phi_2+\alpha_4-\alpha_1-\delta)\\ &-\cos(2\phi_K)\sin(\phi_3-\phi_2+\alpha_4-\alpha_1-\delta)] + \mathcal{O}\left(\sin^2\theta_{13}\right).\end{aligned} \tag{39}$$

No large numerical factors offset the $\sin\theta_{13}$-suppression, so that the modified θ bounds are again as stringent as those exemplified in Fig. 3.

5.3 Scenario II: $\sin 2\phi_K \sim 0$

If $\sin 2\phi_K$ is close to zero, CMM effects cannot make their way into $\text{Im}M_{12}^K$ anymore, and the best constraints on θ are obtained from ΔM_K and B physics observables. As mentioned in Sec. 4, ΔM_K is plagued by hadronic uncertainties, so that we merely impose $|\Delta M_K^{\text{CMM}}| < \Delta M_K^{\text{exp}}$ to stay on the conservative side. In this case, for $m_{\tilde{g}} \simeq 700\,\text{GeV}$, the constraint from ΔM_K only starts to compete with that from $|\epsilon_K|$ when $|\phi_K| = \mathcal{O}(0.1°)$, corresponding to $\theta^{\max} \simeq 10° - 30°$ (depending on the precise values of $\Delta_{\tilde{d}}$ and $m_{\tilde{d}}/m_{\tilde{g}}$). The constraints from ΔM_d, $S_{J/\psi K_S}$, and $\Delta M_d/\Delta M_s$ are in general better, as we illustrate in Fig. 4 for Set 1 and Set 2. The dependence of the contours of the black areas on $\Delta_{\tilde{d}}$ and

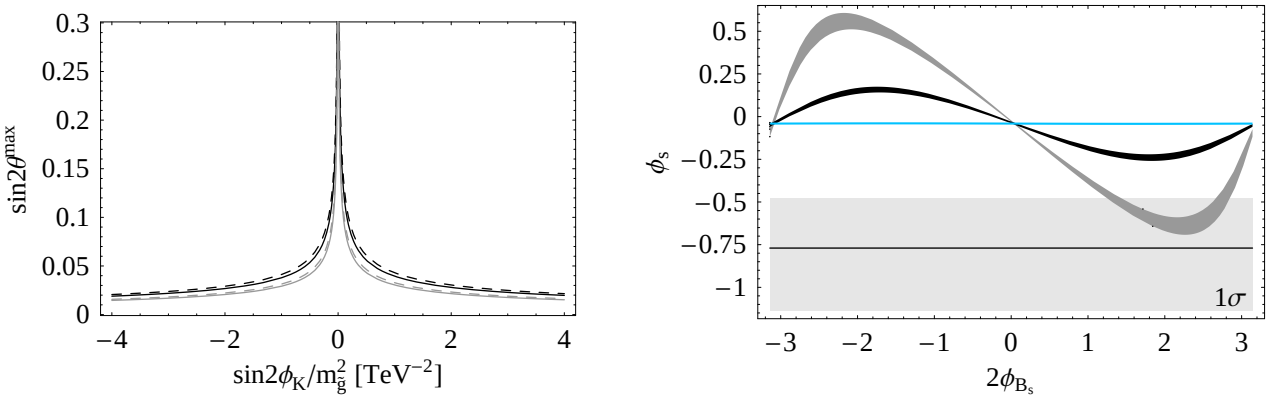

Figure 3: Left: Constraints on θ from $|\epsilon_K|$ as a function of $\sin 2\phi_K/m_{\tilde{g}}^2$ for $\Delta_{\tilde{d}} = 0.46$ (black) / 0.55 (gray) and $m_{\tilde{d}}/m_{\tilde{g}} = 0.47$ (plain) / 0.33 (dashed). Right: CP-violating phase ϕ_s as a function of the CMM phase ϕ_{B_s}. The light gray (dark gray) curve corresponds to Set 1 (Set 2) with $\theta = 0$. The SM prediction (horizontal line) is recovered for $2\phi_{B_s} = 0, \pm\pi$. The broad gray band indicates the one-sigma measurement [23].

$m_{\tilde{d}}/m_{\tilde{g}}$ is similar to the one displayed in Fig. 3-left. Note that the constraint from $\Delta M_d/\Delta M_s$ depends on both ϕ_{B_s} and $\phi_{B_d} = \phi_K + \phi_{B_s}$. The plots shown in Fig. 4 correspond to $\phi_K = 0$ and $\phi_K = \pi/2$. Other ϕ_K values lead to different plots, with however the same general appearance, in particular the exclusion of small θ angles for some specific ϕ_{B_s} values. For these specific values, the tight bounds on θ derived in Sec. 5.2 are thus even surpassed.

As mentioned previously, ϕ_s can cut further into the parameter space, especially for negative ϕ_{B_s} values, see Fig. 3-right. However, this does not change the typical value of $\theta^{\max}$ obtained from B physics observables, which is of ten or a few tens of degrees.

5.4 Closing the Unitarity Triangle

Recently, several studies pointed out a possible tension in the SM between the value of $\sin 2\beta$ predicted from $|\epsilon_K|$ and $\Delta M_s/\Delta M_d$, and its direct measurement from $S_{J/\psi K_S}$ [36, 20, 37, 38]. In this section, we illustrate how CMM effects can remove this tension, and simultaneously account for a sizeable CP-violating phase in the B_s system.

Due to the particular sensitivity of $|\epsilon_K|$ to new-physics effects, either θ or ϕ_K must be very small. We will thus consider the two limits $\theta = 0$ and $\phi_K = 0$. For each case, we will compare the value of $\sin 2\beta$ extracted from $S_{J/\psi K_S}$ with its determination from $|V_{us}|$, $|V_{cb}|$, $|\epsilon_K|$, and $\Delta M_s/\Delta M_d$, obtained inverting the following expressions with respect to $\sin 2\beta$ and R_t:

$$|\epsilon_K| = \kappa_\epsilon \frac{M_K F_K^2 \widehat{B}_K}{12\sqrt{2}\Delta M_K} \times \left\{ \frac{G_F^2 M_W^2}{\pi^2} |V_{cb}|^2 |V_{us}|^2 \left[|V_{cb}|^2 R_t^2 \sin(2\beta)\eta_2 S_0(x_t) \right.\right. \\ \left.\left. + 2R_t \sin\beta \left(\eta_3 S_0(x_c, x_t) - \eta_1 S_0(x_c)\right)\right] - \frac{\alpha_s^2(M_S)}{8m_{\tilde{g}}^2} \sin(2\phi_K) \sin^2(2\theta) \frac{\eta_2\eta_6}{r} S^{(\tilde{g})}(r_1, r_3) \right\}, \tag{40}$$

$$\frac{\Delta M_s}{\Delta M_d} = \xi^2 \frac{M_{B_s}}{M_{B_d}} \frac{\sqrt{\left(k_1 + X\cos 2\phi_{B_s}\cos^2\theta\right)^2 + \left(-2k_2 R_t \sin\beta |V_{us}|^2 - X \sin 2\phi_{B_s}\cos^2\theta\right)^2}}{\sqrt{\left(R_t^2\cos 2\beta |V_{us}|^2 + X\cos 2\phi_{B_d}\sin^2\theta\right)^2 + \left(R_t^2 \sin 2\beta |V_{us}|^2 - X\sin 2\phi_{B_d}\sin^2\theta\right)^2}}. \tag{41}$$

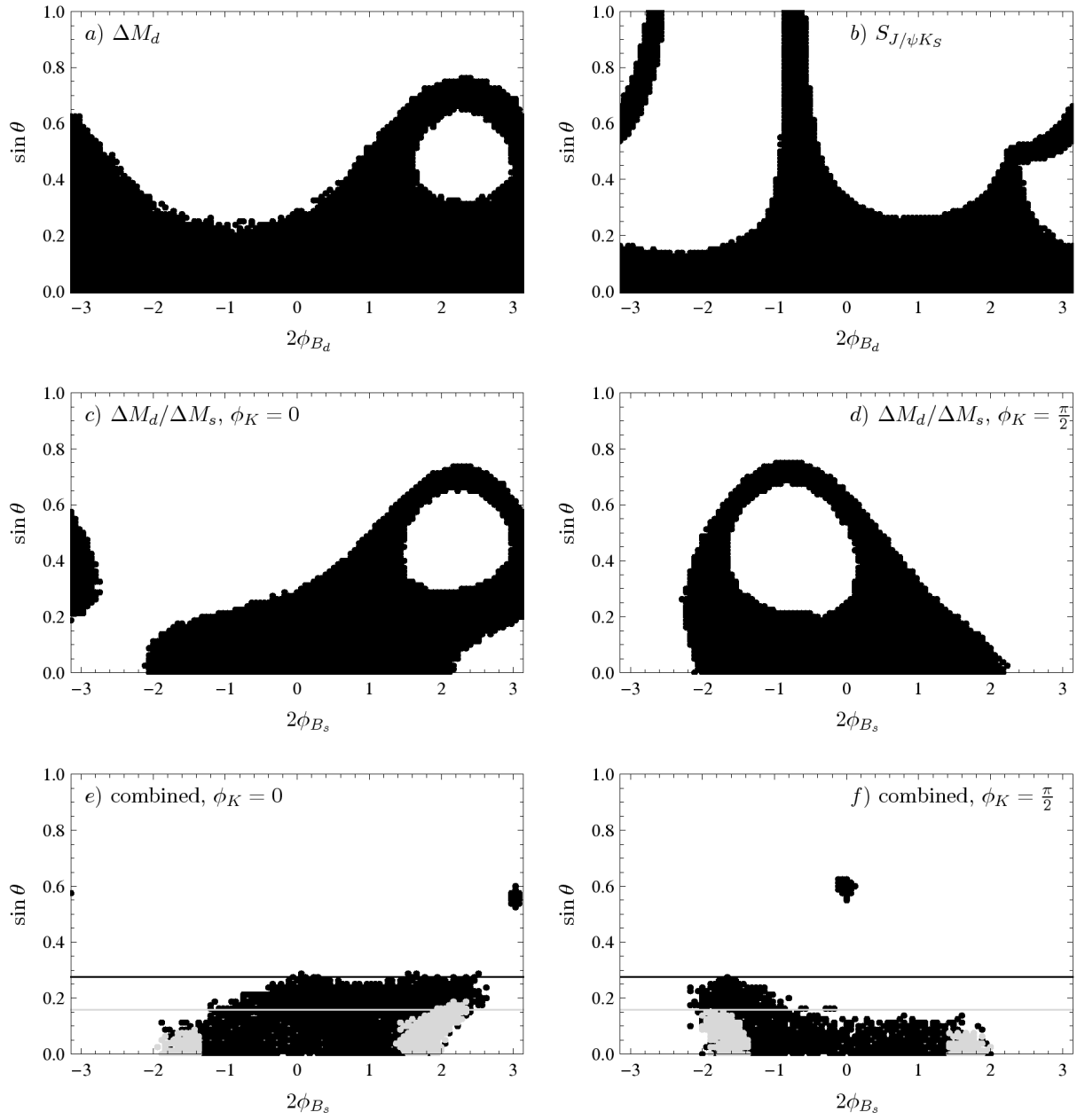

Figure 4: Constraints on θ from B physics observables. Black (gray) points indicate allowed regions in Set 2 (Set 1) parameter space. The first four plots show individual three-sigma constraints from (a) ΔM_d, (b) $S_{J/\psi K_S}$, (c) $\Delta M_d/\Delta M_s$ setting $\phi_K = 0$, (d) $\Delta M_d/\Delta M_s$ setting $\phi_K = \pi/2$. Plots (e) and (f) show the combined (a,b,c) and (a,b,d) constraints, respectively. In the case of Set 1, the three-sigma constraint from ΔM_s has also been imposed, excluding points outside the $1.3 \lesssim |2\phi_{B_s}| \lesssim 2.3$ range (recall that Set 2 is not affected by this constraint). Imposing further the constraint from ϕ_s would remove the gray points with $2\phi_{B_s} < 0$ and the black points with $-2.4 < 2\phi_{B_s} < -1$, see Fig. 3-right. Finally, Set 2 (Set 1) points above the black (gray) horizontal line are excluded by ΔM_K.

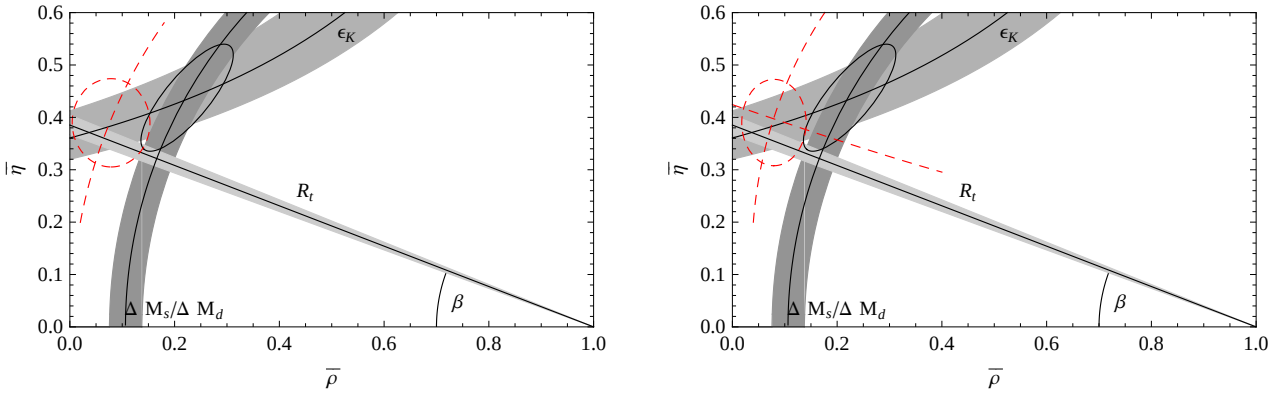

Figure 5: One-sigma constraints on the UT from $S_{J/\psi K_S}$ (light gray), $|\epsilon_K|$ (gray), and $\Delta M_s/\Delta M_d$ (dark gray) in the SM. The one-sigma region determined from $|V_{us}|$, $|V_{cb}|$, $|\epsilon_K|$, and $\Delta M_s/\Delta M_d$ assuming the SM is shown in black, and its shift due to CMM effects is indicated in dashed red. Left: Scenario I, $\theta = 0, \phi_{B_s} = 0.7$. Right: Scenario II, $\theta = 0.1, \phi_{B_s} = \phi_{B_d} = 0.8$. CMM inputs: Set 1.

Here $k_1 = 1 + |V_{us}|^2(1 - 2R_t \cos\beta)$, $k_2 = 1 + |V_{us}|^2(1 - R_t \cos\beta)$,

$$X = \frac{\pi^2 \alpha_s^2(M_S)\, \eta_6\, S^{(\tilde{g})}(r_1, r_3)}{2|V_{cb}|^2 G_F^2 M_W^2 m_{\tilde{g}}^2\, r\, S_0(x_t)}, \tag{42}$$

and $R_t = |V_{td}V_{tb}^*|/|V_{cd}V_{cb}^*|$ is a side of the unitarity triangle (UT). The above expressions hold to 0.5% accuracy. In the SM, this leads to $\sin(2\beta^{\epsilon_K}) = 0.81^{+0.11}_{-0.09}$ with the inclusive $|V_{cb}|$ determination of Tab. 2, and to $\sin(2\beta^{\epsilon_K}) = 0.98^{+0.02}_{-0.11}$ if the exclusive determination from $B \to D^*\ell\nu$ decays, $|V_{cb}|^{\rm excl} = (38.8 \pm 1.1) \cdot 10^{-3}$ [23], is used instead. Note that $|V_{cb}|^{\rm incl}$ does not lead to any significant deviation with respect to $S^{\rm exp}_{J/\psi K_S}$, while a tension is indeed observed with the smaller value $|V_{cb}|^{\rm excl}$. In order to illustrate how CMM effects can compensate for a low $|V_{cb}|$ input in UT analyses, we will adopt the averaged value of Ref. [38], $|V_{cb}|^{LS} = (41.0 \pm 0.63) \cdot 10^{-3}$. In the following, we use the CMM input parameters of Set 1. All errors are treated as gaussian.

$\theta = 0$: CMM effects in R_t Since for $\theta = 0$ there are no effects in K and B_d mixing, CMM contributions enter the UT only via ΔM_s. From Fig. 5-left, one sees that R_t has to increase in order to close the UT. This requires a CP-violating phase $2\phi_{B_s} \in [1.3, 1.8]$, taking into account the three-sigma constraints on ϕ_{B_s} from ΔM_s and ϕ_s. The dashed red curve shows R_t for $\phi_{B_s} = 0.7$, such that the UT determined from $|\epsilon_K|$ and $\Delta M_s/\Delta M_d$ agrees with the $\sin 2\beta$ measurement from $S_{J/\psi K_S}$.

$\phi_K = 0$, $\theta = 0.1$: CMM effects in R_t and β In this second case, CMM effects affect both $\Delta M_s/\Delta M_d$ and $S_{J/\psi K_S}$. For a fixed angle θ, the UT can be closed by adapting the CMM phase $\phi_{B_s} = \phi_{B_d}$. The resulting apex of the UT is shown by the intersection of the dashed red lines in Fig. 5-right for $\theta = 0.1$ and $\phi_{B_s} = 0.8$. For any value of θ allowed by the constraints from B_d and B_s observables in Sec. 5.3, one can find a phase ϕ_{B_s} to close the UT.

Deviations from these two limit cases, i.e., small but nonzero θ or ϕ_K values, rapidly generate CMM effects in $|\epsilon_K|$ as well (Fig. 3-left). These can lower the band from the $|\epsilon_K|$ constraint in the $(\overline{\rho}, \overline{\eta})$ plane, directly making up for the low $|V_{cb}|$ input value.

6 Conclusions

Grand-unified theories introduce relations among quark and lepton masses and mixings. Motivated by the large atmospheric mixing angle in the neutrino sector, several studies focussed on the consequences of the SU(5) Yukawa relation $\mathsf{Y}_d = \mathsf{Y}_e^\top$ in $b \to s$ transitions. In this work, we considered corrections to this relation which are essential to account for the observed light quark and lepton masses. In particular, we investigated the effects on $s \to d$ and $b \to d$ transitions of the additional rotation of the d_R and s_R quarks. This deviation with respect to the PMNS matrix, denoted by U, can be parameterized by an additional mixing angle θ (see Eqs. (11,12)).

In our analysis, we focussed on models with small Higgs representations; a modified version of the CMM model served as our specific scenario. In this setup, the differences between the down-quark and charged-lepton masses are naturally explained by dimension-five Yukawa operators. The associated supplementary rotation θ was constrained from $K - \overline{K}$ and $B_d - \overline{B_d}$ mixing observables. In particular, we found that, in the absence of fortuitous cancellations among the new phases in the matrix U, $|\epsilon_K|$ sets a stringent bound on θ, $\theta^{\max} \sim \mathcal{O}(1^\circ)$. Consequently, in the basis where the charged-lepton Yukawa couplings are diagonal, the matrix $\mathsf{D}_e\widetilde{\mathsf{Y}}_\sigma + \widetilde{\mathsf{Y}}_\sigma^\dagger\mathsf{D}_e + 5\frac{\sigma}{v_0}\widetilde{\mathsf{Y}}_\sigma^\dagger\widetilde{\mathsf{Y}}_\sigma$ (in the notations of Eqs. (5,10)) must be diagonal as well. Barring cancellations, this implies that the flavor structure of the couplings which modify the Yukawa unification must be similar to that of the initial terms. In other words, in the corrected relation $\mathsf{Y}_d = \mathsf{Y}_e^\top + 5\frac{\sigma}{v_0}\,\mathsf{Y}_\sigma$ (Eq. (10)), the three matrices Y_σ, Y_d, and $\mathsf{Y}_e^\top$ must be essentially aligned. Constraints from B physics observables (ΔM_d, $S_{J/\psi K_S}$, and $\Delta M_s/\Delta M_d$) were also analyzed, and shown to imply the looser bound $\theta^{\max} \sim \mathcal{O}(10^\circ)$.

While we have worked out this analysis for a specific GUT model, our results hold in general for models with small Higgs representations. An efficient mechanism is naturally needed to render the mixing among right-handed d-quarks visible. In the CMM model, this mechanism is provided by the fast SO(10) running of the $\tilde{d}_R$ soft mass matrix, which generates the large universality breaking $\Delta_{\tilde{d}}$ at the electroweak scale. Of course, other GUT scenarios could include additional sources of flavor and CP violation inducing effects in $|\epsilon_K|$. These could soften the constraints on θ. Yet they would have to be fairly fine-tuned to cancel the potentially large impact of the corrections from the d_R rotation matrix R_d (Eq. (11)).

Interestingly, the correction operators which are of importance for proton decay but contribute equally to the fermion masses ought to have a different flavor structure in order to be in agreement with the experimental limit [16]. Both types of operators are generically present in GUTs. Hence, our analysis is an important step in establishing a consistent grand-unified model.

Finally, we also considered the possible tension between the value of $\sin 2\beta$ predicted from $|\epsilon_K|$ and $\Delta M_s/\Delta M_d$ in the SM and its direct measurement from $S_{J/\psi K_S}$, raised by the authors of Refs. [20, 36, 37, 38]. We illustrated how CMM effects can remove this tension, and simultaneously reduce the 2.2σ discrepancy observed recently in the $B_s - \overline{B_s}$ mixing phase.

Acknowledgements

We are grateful to Ulrich Nierste for initiating the project and to Waldemar Martens for his help with the *Mathematica* code of Ref. [12]. We also thank Christopher Smith and Scott Willenbrock for useful discussions. This work is supported by the DFG grant No. NI 1105/1-1, by the DFG-SFB/TR9, by the Graduiertenkolleg "Hochenergiephysik und Astroteilchenphysik", and by the EU contract No. MRTN-CT-2006-035482 (FlaviaNet).

Appendix: Loop Functions

$$S_0(x_c) = x_c, \tag{43}$$

$$S_0(x_t) = \frac{4x_t - 11x_t^2 + x_t^3}{4(1-x_t)^2} - \frac{3x_t^3 \log(x_t)}{2(1-x_t)^3}, \tag{44}$$

$$S_0(x_c, x_t) = x_c \left[\log \frac{x_t}{x_c} - \frac{3x_t}{4(1-x_t)} - \frac{3x_t^2 \log x_t}{4(1-x_t)^2} \right], \tag{45}$$

$$F(x,y) = -\frac{1}{(x-1)(y-1)} - \frac{1}{x-y}\left[\frac{x \ln x}{(x-1)^2} - \frac{y \ln y}{(y-1)^2} \right], \tag{46}$$

$$G(x,y) = \frac{1}{(x-1)(y-1)} + \frac{1}{x-y}\left[\frac{x^2 \ln x}{(x-1)^2} - \frac{y^2 \ln y}{(y-1)^2} \right], \tag{47}$$

$$L_0(x,y) = \frac{11}{18} G(x,y) - \frac{2}{9} F(x,y), \tag{48}$$

$$S^{(\tilde{g})}(x,y) = L_0(x,x) - 2L_0(x,y) + L_0(y,y). \tag{49}$$

References

[1] J. C. Pati and A. Salam, Phys. Rev. D **8** (1973) 1240.

[2] H. Georgi and S. L. Glashow, Phys. Rev. Lett. **32** (1974) 438.

[3] H. Georgi, in: *Particles and fields* (ed. C. Carlson), AIP Conf. Proc. **23** (1975) 575;
H. Fritzsch and P. Minkowski, Annals Phys. **93** (1975) 193.

[4] H. Georgi and S. L. Glashow, Phys. Rev. D **6** (1972) 429.

[5] P. Minkowski, Phys. Lett. B **67** (1977) 421.

[6] L. J. Hall and L. Randall, Phys. Rev. Lett. **65** (1990) 2939;
G. D'Ambrosio, G. F. Giudice, G. Isidori, and A. Strumia, Nucl. Phys. B **645** (2002) 155;
G. Colangelo, E. Nikolidakis, and C. Smith, Eur. Phys. J. C **59** (2009) 75;
B. Grinstein, V. Cirigliano, G. Isidori, and M. B. Wise, Nucl. Phys. B **763** (2007) 35.

[7] A. Buras *et al.*, Nucl. Phys. B **592** (2001) 55.

[8] A. H. Chamseddine, R. Arnowitt, and P. Nath, Phys. Rev. Lett. **49** (1982) 970;
R. Barbieri, S. Ferrara, and C. A. Savoy, Phys. Lett. B **119** (1982) 343.

[9] D. Chang, A. Masiero, and H. Murayama, Phys. Rev. D **67** (2003) 075013.

[10] See, e.g., S. Baek, T. Goto, Y. Okada, and K. i. Okumura, Phys. Rev. D **63** (2001) 051701;
T. Moroi, Phys. Lett. B **493** (2000) 366;
R. Harnik, D. T. Larson, H. Murayama, and A. Pierce, Phys. Rev. D **69** (2004) 094024;
J. Hisano and Y. Shimizu, Phys. Lett. B **565** (2003) 183;
M. Ciuchini, A. Masiero, L. Silvestrini, S. K. Vempati, and O. Vives, Phys. Rev. Lett. **92** (2004) 071801;
K. Cheung, S. K. Kang, C. S. Kim, and J. Lee, Phys. Lett. B **652** (2007) 319.

[11] S. Jäger and U. Nierste, Eur. Phys. J. C **33** (2004) S256.

[12] S. Jäger, M. Knopf, W. Martens, U. Nierste, C. Scherrer, and S. Wiesenfeldt, in preparation.

[13] T. Moroi, JHEP **0003** (2000) 019;
N. Akama, Y. Kiyo, S. Komine, and T. Moroi, Phys. Rev. D **64** (2001) 095012.

[14] R. Barbieri, L. J. Hall, and A. Strumia, Nucl. Phys. B **449** (1995) 437.

[15] J. R. Ellis and M. K. Gaillard, Phys. Lett. B **88** (1979) 315.

[16] B. Bajc, P. Fileviez Perez, and G. Senjanovic, Phys. Rev. D **66** (2002) 075005;
D. Emmanuel-Costa and S. Wiesenfeldt, Nucl. Phys. B **661** (2003) 62.

[17] S. Wiesenfeldt, Phys. Rev. D **71** (2005) 075006;
S. M. Barr and I. Dorsner, Phys. Lett. B **632** (2006) 527.

[18] J. A. Casas, A. Ibarra, and F. Jimenez-Alburquerque, JHEP **0704** (2007) 064;
J. Sayre and S. Wiesenfeldt, Phys. Rev. D **77** (2008) 053005.

[19] A. J. Buras, arXiv:hep-ph/0505175; K. Anikeev *et al.*, arXiv:hep-ph/0201071.

[20] A. J. Buras and D. Guadagnoli, Phys. Rev. D **78** (2008) 033005.

[21] A. Lenz and U. Nierste, JHEP **0706** (2007) 072.

[22] C. Amsler *et al.* [Particle Data Group], Phys. Lett. B **667** (2008) 1. Updates on `http://pdg.lbl.gov`.

[23] E. Barberio *et al.* [Heavy Flavor Averaging Group], arXiv:0808.1297 [hep-ex]. Updates on `http://www.slac.stanford.edu/xorg/hfag`.

[24] S. Herrlich and U. Nierste, Nucl. Phys. B **476** (1996) 27.

[25] A. Buras, M. Jamin, and P. Weisz, Nucl. Phys. B **347** (1990) 491.

[26] M. Antonelli *et al.* [FlaviaNet Working Group on Kaon Decays], arXiv:0801.1817 [hep-ph], `http://www.lnf.infn.it/wg/vus/`.

[27] V. Lubicz and C. Tarantino, arXiv:0807.4605 [hep-lat].

[28] M. Battaglia *et al.*, arXiv:hep-ph/0304132.

[29] G. Buchalla, A. J. Buras, and M. E. Lautenbacher, Rev. Mod. Phys. **68** (1996) 1125.

[30] K. Chetyrkin, J. Kühn, and M. Steinhauser, Comput. Phys. Commun. **133** (2000) 43.

[31] I. Allison *et al.*, arXiv:0805.2999 [hep-lat].

[32] Tevatron Electroweak Working Group for the CDF and D0 Collaborations, arXiv:0808.1089 [hep-ex].

[33] J. Charles *et al.* [CKMfitter Group], Eur. Phys. J. **C41** (2005) 1. Updates on `http://ckmfitter.in2p3.fr`.

[34] M. Drees, Phys. Lett. B **181** (1986) 279.

[35] R. Barate *et al.* [LEP Working Group for Higgs boson searches], Phys. Lett. B **565** (2003) 61.

[36] E. Lunghi and A. Soni, Phys. Lett. B **666** (2008) 162.

[37] A. Buras and D. Guadagnoli, arXiv:0901.2056 [hep-ph].

[38] E. Lunghi and A. Soni, arXiv:0903.5059 [hep-ph].